Journal of Materials Science and Engineering B 8 (9-10) (2018) 181-187
doi: 10.17265/2161-6221/2018.9-10.001

Influence of Tungsten and Cobalt Contents on the Microstructure Changes and Fracture Behavior of New Carbon-Free Steel-alloy Composites

W. S. Elghazaly[1] and O. Elkady[2]

1. Steel Technology Dept., CMRDI, PO Box 87, Helwan, Cairo, Egypt

2. Manufacturing Sector, CMRDI, Cairo, Egypt

Abstract: The ever increasing demand for steel materials that have good combinations between strength and toughness urged all researchers working in the field of material science to find new alloys that can approach that requirement. Unfortunately strength and toughness of materials are always counter acting properties. However, carbon contents in the steel define to a great extent its strength and toughness. In this research an effort is paid to produce steel alloy composites that can give higher strength together with good toughness without alloying with carbon. The mechanism of strengthening in Iron-Cobalt-Tungsten composite alloys with variations in Co and W contents is investigated. The fracture toughness and hardness, are measured for all alloy composites under investigation. The changes in microstructures after heat treatment are emphasized using metallurgical microscopy and SEM-aided with EDX analyzing unit.

Key words: Steel alloys, precipitation hardening, carbon-free alloys, fracture toughness, microstructure, strengthening, composite materials.

1. Introduction

Precise machining operations depend on type and durability of cutting tools. Family of cold and hot work tool steels were designed to serve several machining operations as presented in ASTM A681 standards [1]. The as-annealed products of tool steels are soft and workable to the desired shapes of tooling parts which acquire their strength, hot hardness, gouging and fatigue resistance by special heat treatment processes [2, 3]. Near-net shape cast tooling is also applied to form cutting tools which also acquire their properties after heat treatment and cutting edge adjustments [4, 5]. Higher abrasive and adhesive resistance of such cutting tools are obtained by tool alloys containing carbide forming elements as tungsten, vanadium, cobalt and molybdenum as in die and high speed steel tools [6, 7]. The strengthening mechanism of such tool steels depends on the transformation of austenite to martensite along with precipitation of primary and secondary carbides [8]. In all cases, the uneven-coarse distribution of primary and secondary carbides after heat treatment causes loss of cutting performance due to rapid over-aging of carbides at high temperature above 500 °C [9]. Furthermore, the hardening process of such steel alloys causes distortion and may introduce hair cracks in the steel [10].

There are however other strengthening mechanisms that need low temperature such as grain refinement and precipitation of intermetallic compounds in the tool steel matrix. In precipitation hardening for example in superalloys or maraging steel hard intermetallic compounds are attained after isothermal aging process without dimensional changes or distortion [11]. Previous researches have been done to emphasis the role of powder metallurgy in manufacturing high speed tool steel with superior

Corresponding author: Waleed Elghazaly, Ph.D., research field: steel technology.

properties if compared with that produced through conventional steelmaking rout [12, 13].

In this investigation, different alloys of carbon free tool steel composites are produced using iron, cobalt and tungsten powders aiming to study the effect of composition, heat treatment on their microstructures, hardness and fracture toughness.

2. Experimental Procedure

2.1 Materials Processing

Four steel bars 55 × 10 × 10 mm were prepared by consolidation from their powder constituents (iron-Cobalt-Tungsten) by hot isostatic pressing (HIP) at 1,250-1,300 °C and 550 MPa. The powdered constituents were blended in a tumbling mixer in dry basis for 1.5 h and then compacted under 550 MPa uniaxial pressure in a special steel die to final product. The bar samples were then sintered at 1,250-1,300 °C for 3 h under vacuum. The final adjusted composition of the experimental steel composites sinter is shown in Table 1. Some of the sintered bars were forged at 1,380 °C to about 20-40% reduction in thickness to study the differences in densification and porosity distribution if any.

2.2 Heat Treatment

Specimens of sintered steel rods A-1 to A-4 and others forged ones were solution treated (1,150 °C, 30 min, oil quenched). The as-sintered and as-deformed solution treated samples are then aged at 250 to 750 °C for 2 hours and then air cooled to strengthen their matrices by precipitation hardening mechanism through forming series of intermetallic phases. Fig. 1 illustrates the procedure of solution treatment and tempering heat treatment.

Table 1 Chemical composition of sintered tool steel bars.

Element, wt.%	Fe	Co	W	Mn	Si	S	P
A-1	84.82	8	7	0.07	0.10	0.003	0.005
A-2	79.83	10	10	0.05	0.11	0.005	0.004
A-3	74.88	15	10	0.04	0.07	0.002	0.009
A-4	59.89	25	15	0.03	0.13	0.008	0.012

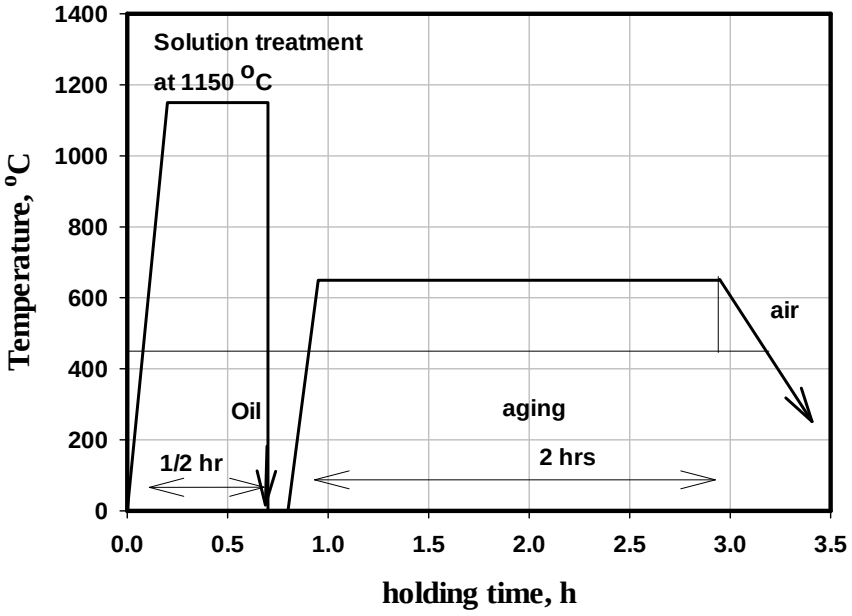

Fig. 1 Heat treatment cycles of experimental tool steels A-1 to A-4.

3. Results and Discussions

3.1 Compactness and Densification

The density and dimensions of the consolidated bars of produced tool steels were subjected to changes during processing depending on the sintering temperature at constant pressure (550 MPa) as shown in Fig. 2. Densities of about 9.7 and 9.8 gm/cm^3 were reached for A-4 (Fe-, 25%Co, 15%W) tool steel under such conditions and at sintering temperatures 1250 °C and 1,300 °C respectively, while shrinkage of about 17-22% in such steel was measured after sintering. The compactness and density of for example A-4 tool steel bars, was upgraded to reach 10.6 gm/cm^3 after 20-40% reduction in thickness by drop forging at 1,380 °C.

3.2 Microstructure Investigation

Cobalt and Tungsten dissolved in liquid Iron to form series of solid solution and intermetallic compounds as shown in the Fe-Co and Fe-W equilibrium phase diagrams Figs. 3a and 3b [14]. The presence of 10-65% cobalt enriched formation of ferrite, while some of austenite could be preferred by addition of tungsten.

The as-sintered microstructures depended to a great extent on the composition of the experimental tool steel as projected in Figs. 4a-4d. A completely clear, interlocked homogeneous microstructure was obtained at compositions Fe-, 25%Co, 10-15%W (Fig. 4b) while the worst microstructure was obtained for alloy compositions Fe-, 8-10%Co, 7-10%W, hence polygonal identified sintered microstructures together with clear grain boundaries were detected in Fig. 4a. The main differences in microstructures revealed the absence of grain boundaries and the increasing homogeneity in case of A-4 tool steel compositions.

At lower cobalt and tungsten contents as in compositions A-1, A-2, it was observed that the presence of grain boundaries dominated the steel matrix field. However, the aged microstructure of steel A-4 was found to be homogeneous with good distribution of phases (ferrite, austenite and μ phase ppts.) as in Fig. 4c. Forging of the sintered steel to 25% reduction in thickness altered the microstructure of steel A-4 to more dense, clear and grain oriented (banded)

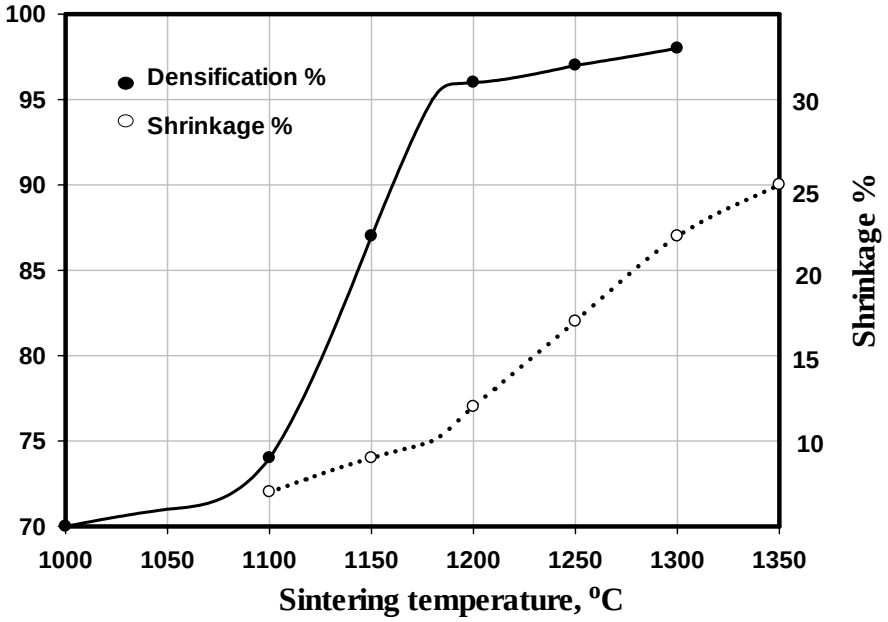

Fig. 2 Dependency of density and shrinkage of A-4 tool steels on sintering temperature at 550 MPa.

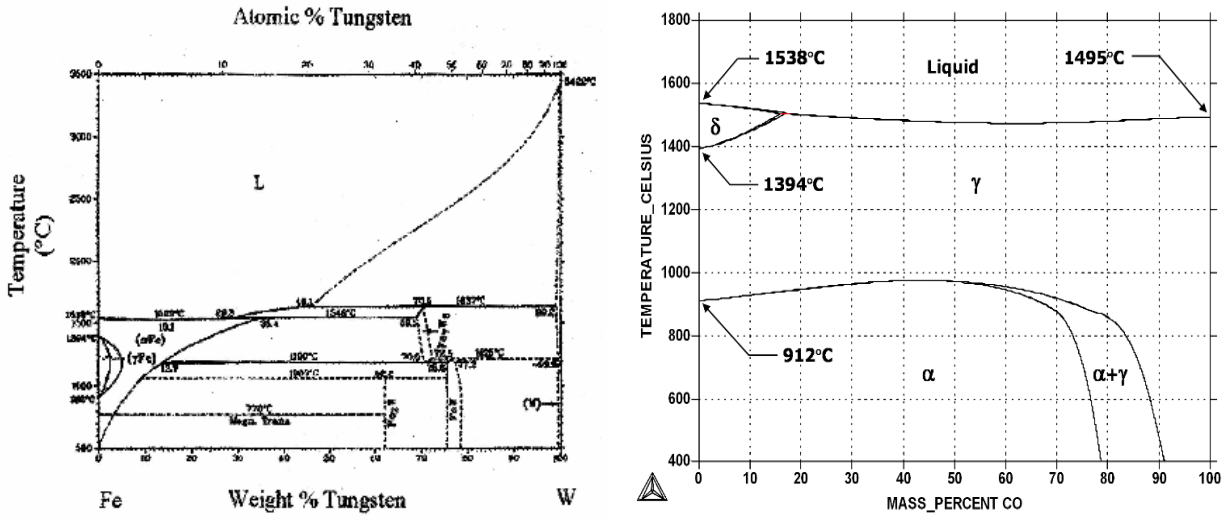

(a) (b)

Fig. 3 Equilibrium phase diagram of Fe-W (a), and Fe-Co (b).

ferrite austenite phases, Fig. 4d, that catalyzed the formation of intermetallic massive precipitation during temper-aging process as shown in Fig. 5b. At lower cobalt and tungsten contents (alloy A-1, A-2) dissolution of grain boundaries was impossible, hence clear and long boundaries were observed at high magnification as in Fig. 5a. In all cases the massive carbide precipitation found in heat treated conventional HSS tool steel, in Fig. 5c, was not found in alloy A-4 after aging.

3.3 Hardness of Experimental Tool Steels

Bulk hardness of all the specimens was measured using Identic Universal Hardness Testing Machine (IUHTM), where all the as-sintered samples of different compositions showed moderate hardness of about 170-200 HB. The maximum hardness value of about 750 HV was measured for solution treated tool steel A-4 after 2 hours aging at 625 °C, while aging such steel at 400 and 900 °C reduced its hardness to about 500 HV as shown in Fig. 6. Unsatisfactory hardness results (350-450 HV) were obtained for solution treated tool steels A-1, A-2, A-3 after aging at temperature volume 450-700 °C for 2 hours. This means that at 25% Co and 15%W massive precipitation of hard intermetallic (μ) phase inside the ferritic austenitic matrix propagated after aging at 625 °C, as depicted in the above mentioned microstructures

3.4 Fracture Toughness Measurements

The alloys under investigation have high volume fraction of intermetallic μ phase hard precipitations, for this reason the Charpy V or U notch cannot give real measurements. Therefore from fracture mechanics point of view the most straight forward parameter to characterize fracture toughness is the critical stress intensity factor (K) or dynamic fracture parameter (K_{id}). A fracture toughness Kc (Pa.$\sqrt{m}$) measurement was made at room temperature by the indentation factor method [15] which can be calculated from the width of crack induced on applying the Vickers Pyramid hardness test as shown in Fig. 7.

A comparison of calculated fracture toughness of produced tool steel A-1 to A-4 as compared with other materials is shown in Fig. 8. It is evident that alloys having content lower than 25%Co+15%W suffer from deteriorated fracture toughness even after tempering, however the fracture toughness for tool steel A-4 reached 190 MP$\sqrt{m}$. This value was increased to reach

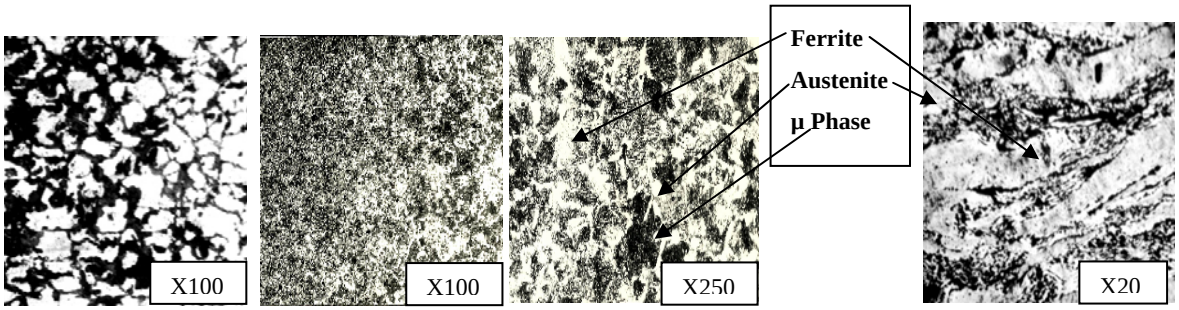

A-1, sintered **A-4, sintered** **A-4, aged** **A-4, forged**

a **b** **c** **d**

Fig. 4 Microstructures of as-sintered, aged and forged aged experimental tool steels.

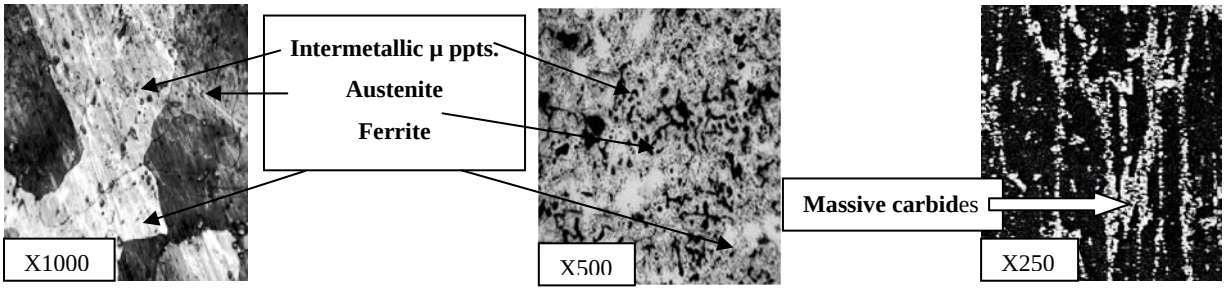

A-4, aged **A-4, forged aged** **HSS [10]**

a **b** **c**

Fig. 5 Microstructures of aged, 25% forged aged A-4, and conventional heat treated HSS.

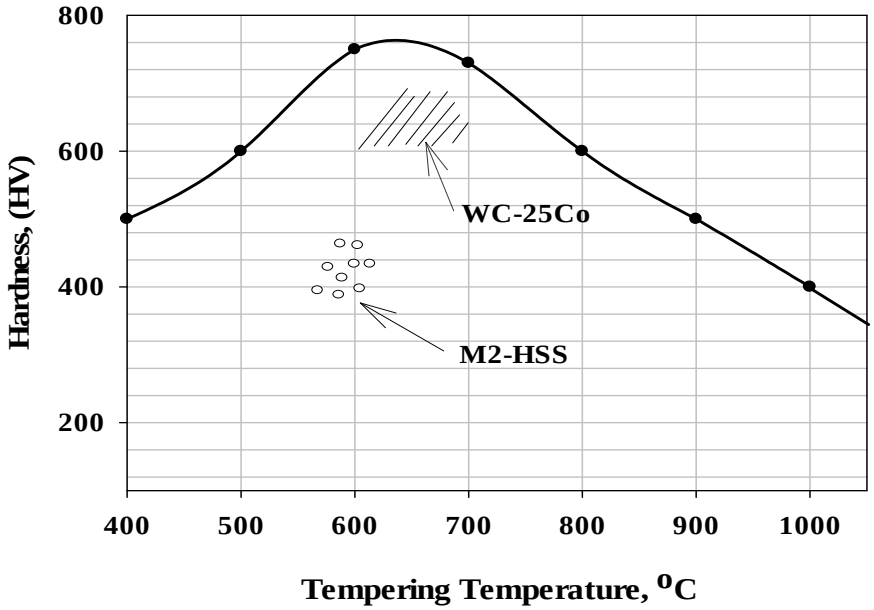

Fig. 6 Relation between hardness of A-4 and tempering (aging) conditions.

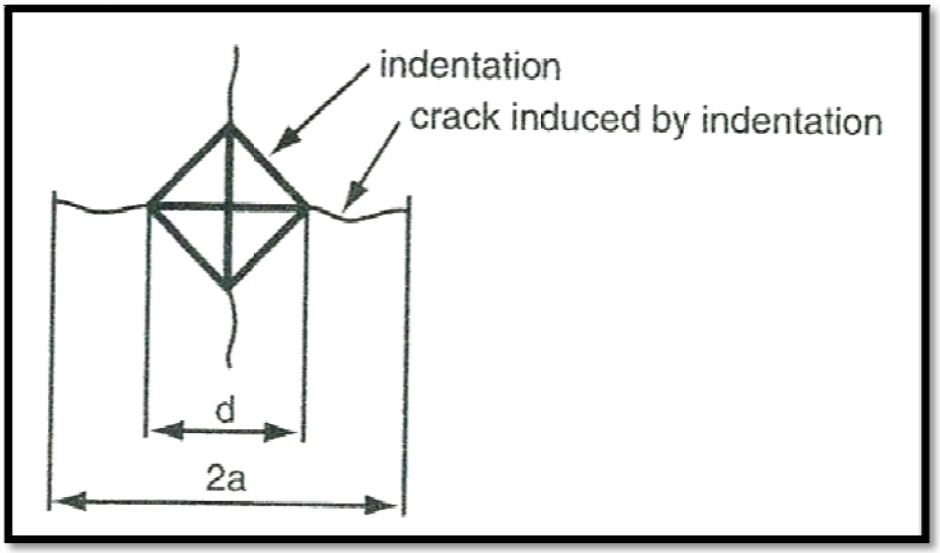

$$Kc = \alpha\sqrt{EP}\ (d/2)/\sqrt[3]{a2}$$

Fig. 7 Hardness vickers indentation test [15].

where: total crack edge distance (m), E = Young's modulus (about 310 GPa), P = load (about 3 N), a half length of crack (m), d = the diagonal length of indentation and α = calibration factor (about 0.025).

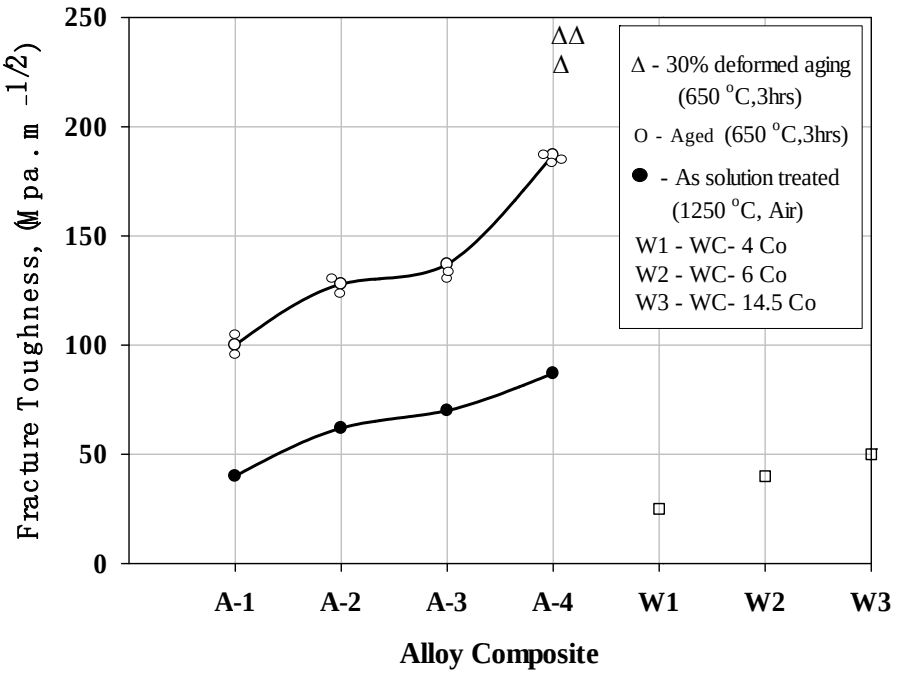

Fig. 8 Fracture toughness values for tool steels as compared with other materials.

about 240 MP$\sqrt{m}$ for A-4 alloy when forged to about 25% thickness and then tempered or aged at the same conditions. This can be attributed to the grain refinement of the alloy matrix due to the strengthening and pinning action caused by both secondary and primary intermetallic μ phase precipitates caused the interaction between Co and W and Fe.

4. Conclusions

(1) Homogeneous interlocked microstructure was obtained at compositions Fe-, 5%Co, 10-15%W, while the worst microstructure was obtained for alloy

compositions Fe-, 8-10%Co, 7-10%W, hence polygonal identified sintered microstructures together with clear grain boundaries were detected. The main differences in microstructures revealed presence of rare grain boundaries and increased homogeneity in case of A-4 tool steel composition.

(2) The maximum hardness value of about 750 HV was measured for solution treated tool steel A-4 after 2 hours aging at 625 °C, while aging such steel at 400 and 900 °C reduced its hardness to about 500 HV.

(3) The fracture toughness of tool steel A-4 reached 190 MP$\sqrt{\boldsymbol{m}}$. This value was increased to about 240 MP$\sqrt{\boldsymbol{m}}$ for A-4 alloy when forged to about 25% thickness and then tempered or aged at 625 °C, while alloys having composition lower than 25%Co+15%W suffered from deteriorated fracture toughness even after age-tempering.

References

[1] *Specifications for Tool Steels*. Online reference found, www.astmsteel.com/ ASTM-A681.

[2] Roberts, G., and Cary, R. 1998. *American Society for Metals*, 5th ed. pp.257-63.

[3] Kumar, K. S., et al. 1991. “Evaluation of As-Hiped PM High Speed Steel Production.” *Met. Metal Trans*. A. 22: 2747.

[4] Takigawa, H., et al. 2013. “Development of Robust Processing Routes for Powder Metallurgy High Speed Steels.” *Powder Metal* 24 (4): 196.

[5] Roberts, G., et al. 1998. *Tool Steels Handbook.* ASM, Materials Park, OH.

[6] Rouzbahani, et al. 2005. “PM-Carbon Free Tool Steel (Fe-Co-Mo).” *Powder Metal Progress* 5 (2): 92.

[7] Sterger, E. 2010. “Influence of Alloying Elements on Precipitation Behavior of Fe-25Co-20Mo Alloy.” Ph.D. thesis, Leoben.

[8] *Boehler Uddeholm Tool Steels Data*, (MC-90 Intermet Alloy), 2013.

[9] El-Ghazaly, S., et al. 1993. “Optimizing Structure, Toughness and Wear-Performance of Cr, Cr+V, Cr+V+Mo Cold Work Cast Tool Steel.” *Steel Research* 64 (2): 136-41.

[10] El-Ghazaly, S. A., and Abbas, M. A. 1991. “Microstructure Analysis of Cast and Forged AISI Mo High Speed Steel.” In *Proceedings of the 2nd International Conference*, Al-Azhar University, Vol. 8, pp. 37-47.

[11] El-Ghazaly, S. A. 1994. “Functionally Graded Mo-HSS.” Presented at the 3rd International Symposium on Structural & Functional Gradient Materials, Lucerne, Switzerland, 10-12 Oct., 1994.

[12] Liu, Z. Y., et al. 2000. “Sintering of Injection Molded M2 HSS.” *Materials Letter* 45: 43.

[13] Danningerm, H., et al. 2013. “Powder Metallurgy of C Free Tool Steels Fe-Co-Mo with Varying Co and Mo Contents.” *Powder Metallurgy Progress* 13 (2).

[14] Web Phase Diagrams for Iron-Tungsten and Iron-Cobalt. http://ispatguru.com/wp-content/uploads/2014/11/Fe-W,Fe-Co.

[15] Yamamoto, K., et al. 2014. “Influence of Mo and Tungsten on High Temperature Hardness of Carbides in White Cast Irons.” *Mat. Trans.* 55 (4): 684.